Japanese Journal of Applied Physics
Vol. 44, No. 7A, 2005, pp. 5244–5248

Electric Field in Solenoids

Soonchil LEE, Yongkwan LEE and Insuk YU[1]

Department of Physics, Korea Advanced Institute of Science and Technology, Taejon 305-701, Korea
[1]*School of Physics and Nano-Systems Institute (NSI-NCRC), Seoul National University, Seoul 151-747, Korea*

(Received July 31, 2004; accepted January 19, 2005; published July 8, 2005)

The time-varying electric field inside a solenoidal coil is measured using a new sensor that minimizes the field disturbance. The experimental results clearly indicate that the main field inside a solenoidal coil is not in the azimuthal direction, but in the axial direction. It is shown that this axial field is generated by surface charges, which are formed to cancel the inductive field inside a conducting wire. [DOI: 10.1143/JJAP.44.5244]

KEYWORDS: electric field, solenoid, surface charge, electric field sensor, field disturbance, inductive field, capacitive field

1. Introduction

It is interesting that there have been many contradictory analyses, even in this decade, to the simple question: Is the ac electric field inside a current-carrying solenoid along the coil axis direction or the azimuthal direction? In 1927, Thomson[1)] argued that the electric field inside a solenoid mainly consists of the induced field that rotates around the coil axis. Townsend and Donaldson[2)] refuted Thomson's argument next year and claimed that the main field is along the axial direction. Later, Townsend and Donaldson's claim was restated by Contaxes and Hatch[3)] in 1969 on the basis of circuit theory. In 1991, Harmon[4)] published a report that contradicted this circuit-theory-based argument. More recently, Henjes[5)] reported a theory that again supports the result of circuit theory. Whatever their results were, none of them clearly recognized the fact that surface charge plays the most important role.

Generally, charge accumulates on the surface of a current-carrying wire although the net amount is usually very small. When a dc current flows in a wire, the surface charges generate an electric field inside the wire that makes the current flow ohmically. This field is uniform in a straight wire. The distribution of the surface charges changes with the geometry of the wire even when the voltage source and the wire remain the same. A handful of reports have already been published aiming to show theoretically and prove experimentally that surface charge is necessary to make current flow.[6)] In fact, the existence of surface charge in a current-carrying wire has been recognized since a long time ago, at least since 1932,[7)] but many discussions have reappeared after Merzbacher's puzzle was proposed in 1980.[8)] Since few physicists have paid attention to this simple classical problem, incorrect descriptions were found even in some famous textbooks, which were corrected after a paper pointed them out.[9)]

When an ac current flows in a wire, on the other hand, the charges in the wire move in response to the total electric field; the sum of the capacitive electric field generated by the surface charges and the electric field induced by the changing magnetic field. From Ohm's law, the current density $\boldsymbol{j}$ in this situation is expressed by

$$\rho \boldsymbol{j} = \boldsymbol{E}_{\mathrm{C}} + \boldsymbol{E}_{\mathrm{I}}, \tag{1}$$

where ρ is the resistivity of the wire, and $\boldsymbol{E}_{\mathrm{C}}$ and $\boldsymbol{E}_{\mathrm{I}}$ are the capacitive and inductive fields, respectively. If the driving voltage and resulting current have a simple harmonic form in time with angular frequency of ω, integration of this equation along the wire gives

$$IR = V_{\mathrm{C}} + iI\omega L, \tag{2}$$

where I, R, and L are the current, resistance, and inductance of the wire, respectively. The integration of the capacitive field due to surface charge, V_{C}, becomes the same as the driving voltage. If the reactance ωL of the coil is much larger than its resistance, i.e., if the quality factor $Q = \omega L/R$ of the coil is much larger than unity as in many solenoids, the LHS of eq. (2) is negligible compared with the second term on the RHS. This implies that $iI\omega L \approx -V_{\mathrm{C}} \gg IR$, i.e., the inductive field is almost completely cancelled by the capacitive field generated by the surface charges oscillating at the same frequency as the fields in the wire.[10)] In other words, the electric field inside the wire of a solenoid is always almost zero at high frequencies, in contrast to the dc case. This is an important point which should be considered in the theoretical analysis of ac electric fields near a coil.

The consequence of this fact is obvious in the case of solenoidal coils. The inductive field, which is in the azimuthal direction in solenoids, is cancelled by the azimuthal component of the capacitive field inside the wire. The cancellation is perfect if the wire is perfectly conducting. Outside the wire, on the other hand, the induced field is, generally, not cancelled by the capacitive field. The azimuthal component of the total field is zero on the surface of a perfectly conducting wire due to the boundary conditions of the electric field, and the degree of cancellation decreases with increasing distance from the wire surface. Therefore, the main electric field inside solenoids should consist of the axial and/or radial components of the capacitive field due to surface charges.

In the following sections, we will show experimental evidence for these arguments. Since the exact solution of the surface charge distribution is only available for an infinitely long straight wire, we cannot quantitatively compare experimental and theoretical results in the case of a solenoid. Therefore, we first work on a single-turn ring coil for which an approximate distribution of surface charge can be guessed more easily than for a solenoid. It will be shown that the agreement between theory and experiment is satisfactory for the single-turn ring coil. The information on the near-field distribution of a single-turn ring coil provides us with a better understanding of that of a solenoidal coil.

Among the required properties of an electric field sensor for near-field sensing, field nondisturbance is the most

important. Most of field disturbance of a sensor results from the conducting parts of the probe and from the transmission line connecting the probe to monitoring instruments. To reduce the field disturbance resulting from a probe, several electroptical sensors and techniques have been developed to replace the conventional purely electrical sensor, a dipole antenna. To reduce the field disturbance originating from the transmission line, resistive lines or optical fibers are used in place of coaxial cables for purely electrical sensors or electroptical sensors, respectively. The possibility of studying the electric field of solenoidal coils by using the resonance signal of piezoelectric materials has been reported.[11,12] In this work, the electric field is measured using a new type of sensor we developed using the piezoelectric and converse piezoelectric resonances.[13] This sensor minimizes field disturbance because it has no conducting parts at all. The probed signal, which is proportional to the electric field, is transmitted to a monitoring system neither electrically nor optically, but mechanically through a transmission rod.

2. Experiment

Since the operation principle of the field sensor and detailed experimental procedure can be found in the report on our earlier work,[13] only a brief description is given here. The sensor consists of two quartz disks attached to the opposite ends of a quartz rod (Fig. 1), respectively, which are identical except for the fact that one has electrodes while the other does not. The mechanical oscillation excited in the electrodeless disk by the electric field (the converse piezoelectric effect) is transmitted through the rod to the other quartz disk at the opposite end. A quartz rod of 30 cm length and 4 mm diameter was used as a transmission medium for mechanical oscillation because of its high transmission efficiency. The quartz rod is sufficiently long to allow the quartz disk with electrodes to be placed far away from the region of interest so that the electrodes do not disturb the field. The mechanical oscillation transmitted to the second quartz disk generates a voltage difference between the electrodes coated on the disk (the piezoelectric effect).

The quartz disks are AT-cut resonators of 8.5 mm diameter and 0.5 mm thickness. The reason for choosing AT-cut quartz from many other piezoelectric materials is that it is easily available because quartz crystals are most widely used material for resonators. AT-cut quartz is obtained by cutting quartz parallel to the crystallographic X axis and at $35°15'$ with respect to the Z axis. Therefore, it can be used to measure the electric field component along the Y axis, which is $35°15'$ off with respect to the direction normal to its plane. The three signals obtained at a given position for three different noncopolar Y axis directions can be used to calculate the amplitude and direction of the field at that position.

A schematic diagram of the experimental setup is shown in Fig. 1. The operating rf frequency, 3.92 MHz, was chosen to be the same as the resonance frequency of the quartz disks. The second quartz disk with electrodes is located in a shielded box to minimize direct pick up of the rf field, and the preamplifier is connected directly to the box without any transmission line. A modulation and lock-in detection technique is used to further reduce the noise resulting from the rf pickup.

The rf coil is either a single-turn ring coil or a solenoid. The single-turn ring coil of 17 cm diameter is made of 1 mm diameter copper wire. The lead is placed perpendicular to the ring and connected to a tuning capacitor located 7 cm away from the ring. By adjusting the position and direction of the tuning capacitor, it is possible to decrease the field disturbance of the capacitor to less than the experimental uncertainty, which is about 3%. The solenoid is of 5.0 cm diameter and 7.2 cm length. The pitch between neighboring turns is 0.5 cm and the total number of turns is fifteen. It is wound with the same copper wire as the single-turn ring coil and is connected to the tuning capacitor in the same way.

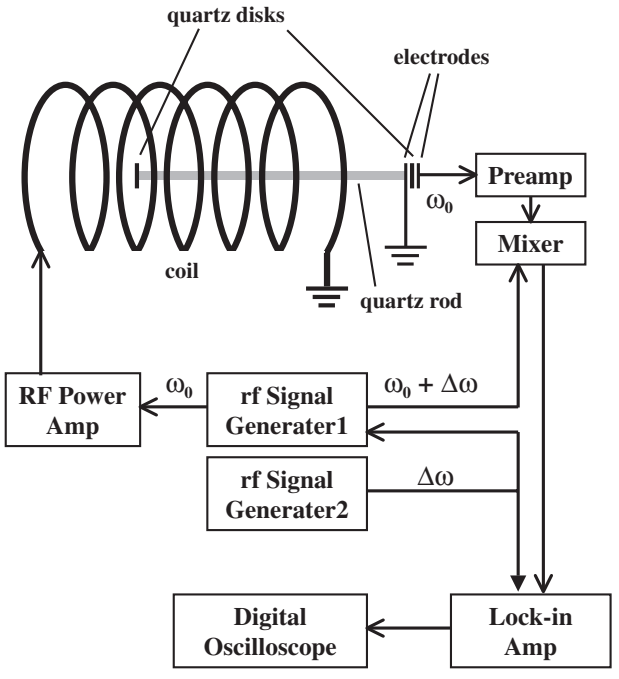

Fig. 1. Schematic diagram of experimental setup and electric field sensor.

3. Results and Discussion

3.1 Electric field from single-turn ring coil

The inductive field generated by the changing magnetic field of the coil should be proportional to the current and in the azimuthal (θ) direction. The strength of the field is independent of θ except at the powered ends ($\theta = 10$ and 350°) where the leads are connected (Fig. 2). However, the

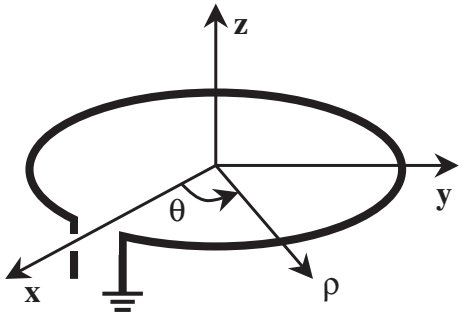

Fig. 2. The single-turn ring coil and coordinate system we used. The grounded and hot ends are designated by the angles $\theta = 10$ and 350°, respectively.

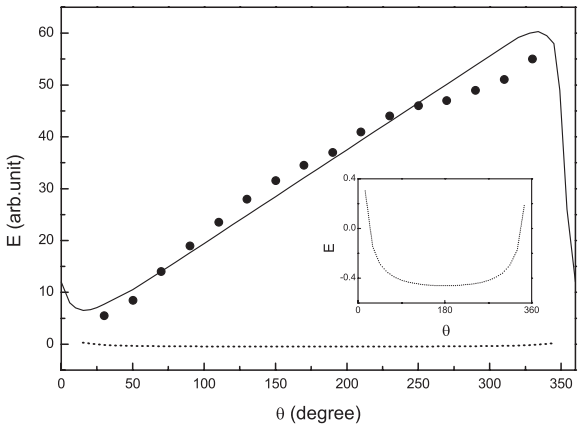

Fig. 3. Azimuthal (θ direction) and perpendicular components of electric field from single-turn ring coil as a function of angle θ. The solid circles are the experimentally measured perpendicular components and the solid and dashed lines are the theoretical predictions of the perpendicular and azimuthal components, respectively. The inset is an expanded view of the azimuthal component. The sign of the azimuthal component is positive when it is in the direction of increasing θ.

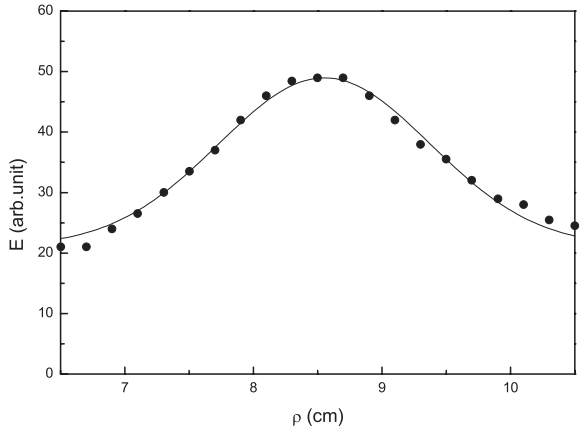

Fig. 4. Perpendicular electric field component from single-turn ring coil as a function of distance from the center of the coil. The radius of the ring is 8.5 cm. The solid line is the numerical result fitted to the data.

experimental results show that the θ component of the electric field is zero near the wire surface within experimental error, while the component perpendicular to the wire surface is much larger, as shown in Fig 3. Hereafter, the perpendicular field always represents the field component perpendicular to a wire surface irrespective of coil geometry. This large perpendicular component of the electric field proves the existence of surface charges since the inductive field cannot provide this component. The absence of the θ component implies that the inductive field is cancelled by the capacitive field.

Although the surface charge distribution is not readily available theoretically for this geometry, it can be obtained experimentally from the perpendicular component of the electric field on the surface of wire because the electric field is proportional to the surface charge on a conducting surface. The perpendicular component shown in Fig. 3 was measured at places just above the ring as a function of the angle θ. The sensor measures the field averaged over its area. Since the probe diameter (8.5 mm) is much larger than the wire size (1 mm), the absolute value of the measured field would be very different from that of the real field on the wire surface. However, this would only influence the proportionality factor in the angle θ dependence of the field strength. Therefore, the approximately linear increase of the field with the angle θ shown in Fig. 3 implies that the surface charge also increases linearly with θ except at the ends. This linear dependence on the angle resembles the case of an infinitely long straight wire where a linear charge distribution is known to be generated to form a constant field inside the wire.[14)]

Since an exact analytical solution is not available for a ring coil, it may be worthwhile numerically clarifying whether the charge density increasing linearly with the angle really generates a constant field inside the ring. We attempted an elementary estimation of the capacitive field inside the wire of a ring coil by numerically summing up the Coulomb fields of a finite number of surface charges,on the basis of a simple assumption that the charge density increases linearly with the angle θ from the end where the coil is grounded. This assumption is definitely not valid near the ends of the coil where the inductive field varies abruptly, and the capacitance of the coil is not negligible. The numerical results are plotted in Fig. 3 together with the experimental data. The perpendicular component of the electric field increases almost linearly with θ, except near the ends of the coil, and changes abruptly in the small gap of the ends. The numerical plot is a fit to the experimental data. The inset of the figure also shows that the linear charge distribution generates an almost constant azimuthal component of electric field inside the wire excluding the vicinity of the ends. This supports the argument that the surface charge is generated to cancel the inductive field of a coil. The abrupt change near the ends of the coil implies that the charge distribution is not linear near the ends. It is worthwhile noting that the amplitude of the θ component is less than 2% of that of the perpendicular component on the surface of the wire at $\theta = \pi$. Therefore, the θ component of the electric field is not detected because of two reasons: the θ component of the capacitive field is cancelled by the inductive field and the component itself is much smaller than the perpendicular component. The surface charge accumulates to cancel the inductive field inside a wire and, at the same time, it generates a perpendicular field that is two orders of magnitude larger outside the wire.

In Fig. 4, the perpendicular component is plotted as a function of the distance ρ from the center of the coil. It is measured at a fixed angle $\theta = \pi$, where the end effect is minimal, and 1 cm above the plane of the ring coil. The field strength is weaker inside the ring coil than outside because the fields due to the surface charges are partly cancelled inside. In the figure, the result of a numerical calculation based on the charge distribution linearly increasing with the angle θ is also shown. The experimental data fits the numerical result well over the entire range of the experimental values. This provides additional evidence for the presence of an approximately linearly increasing charge distribution along the ring.

3.2 Electric field from solenoidal coil

The experimental results on a solenoidal coil are illustrated in Fig. 5. The figure shows the electric field

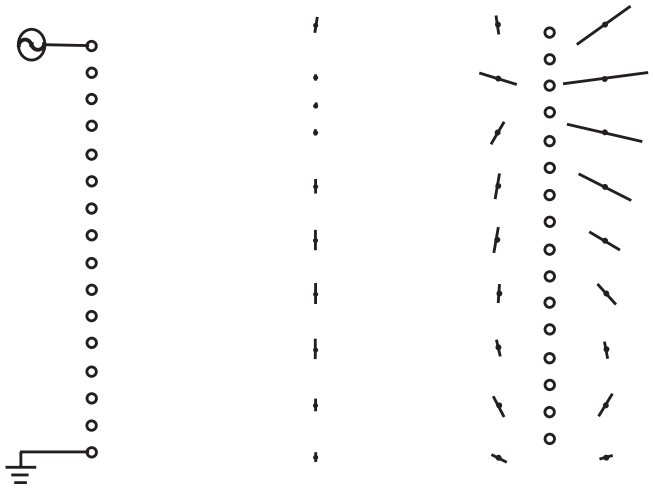

Fig. 5. Schematic view of electric field distribution near solenoidal coil. The open circles represent the cross section of the wire, and the solid lines represent the oscillating electric field vectors measured at each point of the black dots.

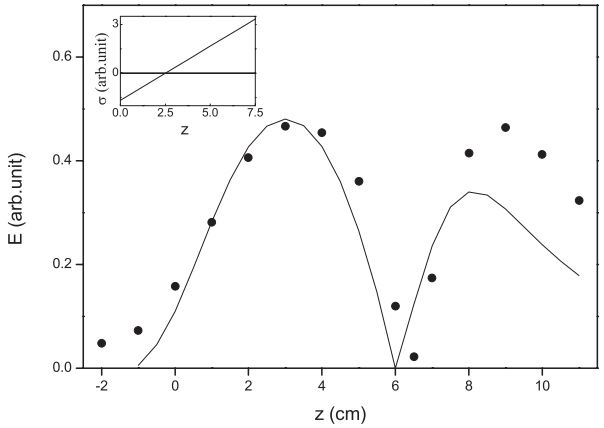

Fig. 6. The axial field amplitudes measured through the solenoid axis (solid circles) are plotted as a function of the distance z from the bottom (grounded end) of solenoid. The grounded and hot ends of the solenoid are placed at $z = 0$ and 7.2 cm, respectively. The solid line is the numerical fit to the experimental data calculated using the linear charge distribution shown in the inset.

distributions on the central cross-sectional plane of the solenoid. The hot and ground leads are on the left side, at the top and bottom of the solenoid, respectively. No azimuthal component is observed either inside or outside the solenoidal coil within experimental error. Therefore, as in the single-turn ring coil, the electric fields shown in Fig. 5 are generated by surface charges. The field strength is generally weaker inside the solenoid than outside, as for the single-turn ring coil, because the fields due to the surface charges, particularly the radial components, are largely cancelled inside. Inside the solenoid, the field directions are mostly axial except near the ends. The radial component decreases rapidly approaching the axis of the solenoid, while the axial component remains relatively constant. On the axis of solenoid, the field direction is purely axial except near the hot end, as it should be considering the symmetry of the coil. Near the hot end, the field direction is a little bit tilted due to the dense surface charge on the lead of the hot end.

The surface charge distribution can be obtained experimentally from the perpendicular field components measured near the surface of the solenoid wire, as for the single-turn ring coil. However, in contrast to the single-turn ring coil, the field near the wire surface is not perpendicular to the surface because of the neighboring turns of the solenoid. Unless the field probe is much smaller than the wire diameter, the field measured near the wire surface is not exactly proportional to the surface charge density. A rough sketch of the surface charge distribution can be obtained from the perpendicular field distribution near the solenoidal wall in Fig. 5. It is noticed that the perpendicular components of the field inside and outside the solenoid change sign crossing zero around 1.5–2.5 cm above the grounded bottom end (the third and fifth points from the bottom). After the zero crossing, the perpendicular component increases with height except near the ends. This means that the surface charge decreases with height from the bottom ring until it reaches zero and, after that, the sign of charge changes and the density increases with height.

We attempt an analysis similar to that for the single-turn ring coil using this observation. The field inside and outside a solenoid is simulated on the basis of the simple assumption that the charge distribution changes linearly with the distance from the grounded end of the solenoid. Since the variation of surface charge with angle should be negligible compared with that with height, we approximate the solenoid as a stack of the same number of coaxial ring coils. Each coil is assumed to have a uniform charge density that increases linearly with the height of the coils. That is, the function adopted to represent this simplified charge distribution is $\sigma = \sigma_0(z - z_0)$ (the inset of Fig. 6). As an example of the comparison of theory with experiment, the axial component on the axis of the solenoid calculated using this charge distribution with $z_0 = 2.5$ is plotted in Fig. 6 as a function of the height z together with the experimental result. The grounded and hot ends of the solenoid are located at $z = 0$ and 7.2 cm, respectively. The experimental result shows that the axial field has two peaks, one near the center of the solenoid (3 cm) and the other above the hot end (9 cm). The axial component of electric field becomes zero near the hot end (6.5 cm). These features are well predicted by the theoretical model based on the simple assumption of a linear charge distribution. The axial fields generated by surface charges at different rings are cancelled at the zero field position and the sign of the total axial field changes crossing this position.

The simulation predicts a zero field position that is a little different from the experiment. In the simulation, z_0 can be varied as a parameter to generate a better fit to the data. As z_0 is increased in the numerical calculation, the position of the zero axial field also moves up, resulting in a better fit to experimental data as far as the zero field position is concerned. However, as z_0 is increased, the total surface charge decreases and the outside field decreases faster than that inside, contrary to the experimental data showing similar peak heights inside and outside. This implies that the surface charge near the hot end is denser than that expected under the assumption of a linear charge distribution, due to the capacitance between the leads that was completely neglected in the simulation, in accordance with a previous report.[11)]

In summary, we have observed that the capacitive electric field component, which is nearly perpendicular to the inductive field, is dominant inside a single-turn ring or a solenoid coil. The surface charge accumulates to cancel the inductive field and, at the same time, generates a perpendicular field that is two orders of magnitude larger. The major field component inside a solenoid is confirmed to be the axial field.

Acknowledgement

This work was supported by the NRL program, eSSC at POSTECH and the Nano-Systems Institute (NSI-NCRC) program sponsored by the Korea Science and Engineering Foundation (KOSEF).

1) J. J. Thomson: Philos. Mag. **4** (1927) 1128.
2) J. S. Townsend and R. H. Donaldson: Philos. Mag. **5** (1928) 178.
3) N. Contaxes and A. J. Hatch: J. Appl. Phys. **40** (1969) 3548.
4) G. S. Harmon: J. Appl. Phys. **69** (1991) 7400.
5) K. Henjes: J. Appl. Phys. **79** (1996) 21.
6) See, for example, R. N. Varney and L. H. Fisher: Am. J. Phys. **52** (1984) 1097.
7) C. Schaefer: *Einfuhrung in die theoretische Physik* (Walter de Gruyter, Berlin, 1932) Vol. 3, Part 1, p. 175 [in German].
8) E. Merzbacher: Am. J. Phys. **48** (1980) 178.
9) B. R. Russell: Am. J. Phys. **36** (1968) 527.
10) M. A. Heald: Am. J. Phys. **56** (1988) 540.
11) D. G. Hughes and L. Pandey: J. Magn. Reson. **56** (1984) 428.
12) K. Choi and I. Yu: Rev. Sci. Instrum. **60** (1989) 3249.
13) D. Lee and S. Lee: Rev. Sci. Instrum. **67** (1996) 3320.
14) A. Marcus: Am. J. Phys. **9** (1941) 225.